Satellite Inertia Estimation and Observability Analysis

Guido Magnani, Hélène Evain, Stéphanie Delavault

DOI: 10.13009/EUCASS2022-6092
9TH EUROPEAN CONFERENCE FOR AERONAUTICS AND SPACE SCIENCES (EUCASS)

Satellite Inertia Estimation and Observability Analysis

MAGNANI Guido, EVAIN Hélène*† and DELAVAULT Stéphanie**
**CNES, Toulouse, France (e-mail: name.surname@cnes.fr)*
†Corresponding author

Abstract
Fine knowledge of the inertia matrix can be crucial to achieving attitude control performance for agile satellites. Moreover, for missions that do not plan inertia calibration manoeuvres, such as the CNES Microcarb mission, the performance of the estimation is directly linked to the inertia's observability during mission guidance manoeuvres. In this context, first two identification methods are compared: the Instrumental Variable (IV) and the Unscented Kalman Filter (UKF). Then, observability metrics are analysed to identify the best range of the dataset suitable for inertia estimation. Finally, we deduced a process based on observability analyses and identification to perform the estimation.

1. Introduction

The inertia matrix typically varies during the satellite lifetime mainly due to fuel consumption. The importance of an accurate identification arises especially for agile satellites, where control laws are sometimes designed directly proportional to the inertia matrix [1] to meet stringent performance constraints. Indeed, even though the control loop can be robust to a larger set of inertia values, ensuring it to remain below a given threshold can significantly reduce the stabilization period and the oscillations after the manoeuvre. Moreover, for instance in the CNES mission Microcarb, there are no specific manoeuvres devoted to the estimation of the inertia matrix. The typical mission guidance manoeuvres performed by the satellite have then to be analysed prior to the estimation process, in order to identify which of them are the most suitable to be used as input in the identification process.

The literature on satellite parameters' estimation, and in particular the inertia, consider at first the least squares method based on the angular momentum conservation [2]. Constraints on the positivity of the inertia matrix and on the diagonal elements have been added in [3] to ensure physically feasible inertia values. The least squares method is mainly used for on-ground estimation even if it can also fit for on-board calculations [3] and [4]. On the other side, the Kalman Filter is suitable for on-board estimation and implementations have been proposed in the literature. For instance [5] designed an Extended Kalman Filter for estimating parameters in the case of a gyroless satellite. Unscented Kalman Filters have also been studied for this problem like in [6] where optimal manoeuvres are designed, or [7]. For on-ground inertia estimation, in order to avoid the bias of the least squares method, an Instrumental Variable method has been implemented in [8] which considers the gyroless satellite problem and uses the dynamics equation of motion. Other typical works on this topic include adaptive control to compensate for the errors, whether by determining directly or not the inertia matrix [9].

The second topic used in this study is the characterization of the observability that a given manoeuvre can provide to ensure a valid estimation. A state of the art of experiment design can be found in the works in particular of [10] and [11] from which criteria can be used to assess the observability of a given set of data. In particular, the A-optimality, E-optimality, D-optimality numbers and Condition Number Optimization on the Fisher information matrix are typical criteria used for the optimization in experiment design. [7] designs nonlinear trajectories using pseudo-spectral optimal control minimizing the condition number of the Fisher matrix. [12] uses a cubic spline parametrization and different cost functions based on the numbers mentioned here above are compared.

In this work, two identification methods are implemented: the Instrumental Variable (IV) designed in a previous work [8] with CRAN University of Lorraine and Région Lorraine, and an Unscented Kalman Filter. The IV method has been selected because it enables remaining consistent with a larger variety of noises than the least squares method and other associated methods. Also, it has been developed with the dynamics equation and adapted to the gyroless case. In addition, in our case, the on-ground estimation is looked for.
The UKF has been selected because, as explained in [13], it enables propagating the Gaussian noise of the system in a more representative way, using sample points that characterize the distribution of the noise. The EKF needs linearized

DOI: 10.13009/EUCASS2022-6092

equations of measurement and of propagation and uses the derived matrices for noise propagation. The UKF seems a more suitable algorithm for systems where linearization can lead to high errors. One drawback is that numerous parameters need to be tuned, and it is difficult to find physical or mathematical justifications. It is often empirical. Nevertheless, for the reasons explained above, the UKF has been selected.

The use case is the Microcarb satellite in development at CNES where no specific inertia identification manoeuvre can be performed. However, since the satellite is agile, different classical criteria [10], [11] used to define optimal manoeuvres are tested in this paper and identification methods are compared in order to derive the most appropriate one. The goal is to find the most observable set of guidance laws for inertia identification.

The next section is dedicated to the description of the inertia estimation methods. Then, the observability metrics are described. In the fourth section, the Microcarb application is explained. The fifth section focuses on comparing and validating the two identification methods on a theoretically well-observable maneuver. Finally, the observability of the input data to use for the estimation is studied. The paper ends with a conclusion and perspectives for future work.

2. Description of the identification methods

2.1 Satellite attitude dynamics

The matrices are written in bold letters and the vectors in upper cases.
The rotational dynamics of a rigid body, expressed in the body reference frame, is described by Euler's equation:

$$T_{ext} = \boldsymbol{I_{TOT}}\dot{\Omega}(t) + \Omega(t)\wedge\boldsymbol{I_{TOT}}\Omega(t) + \dot{H}_{RW}(t) + \Omega(t)\wedge H_{RW}(t) \quad (1)$$

where:

- T_{ext} are the external torques applied to the system
- $\boldsymbol{I_{TOT}}$ is the inertia matrix of the satellite,
- $\Omega(t)$ and Ω_{RW} are the angular rates of body and reaction wheels respectively,
- $H_{RW}(t)$ is the reaction wheels angular momentum
- $\dot{H}_{RW}$(t) is the reaction wheels created torque
- $\wedge$ is the cross-product sign

From this equation, the goal of the estimation method is to calculate $\boldsymbol{I_{TOT}}$ **:**

$$\boldsymbol{I_{TOT}} = \begin{bmatrix} I_{11} & I_{12} & I_{13} \\ I_{12} & I_{22} & I_{23} \\ I_{13} & I_{23} & I_{33} \end{bmatrix}_{R_b}$$

With

- R_b the body reference frame

For some satellites including Microcarb, the solar panel is rotating, inducing a variation of inertia as described below:

$$\boldsymbol{I_{TOT}}(\theta_{SP}) \approx \boldsymbol{I_{CB}} + \boldsymbol{I_{SP}}(\theta_{SP}) \quad (2)$$

where :

- θ_{SP} is the solar panel angle with respect to the satellite base,
- $\boldsymbol{I_{CB}}$ is the cental body inertia,
- $\boldsymbol{I_{SP}}$ is the solar panel inertia.

It should be noted that in the body frame, $\boldsymbol{I_{CB}}$ is constant.

2.1 Instrumental variable method

The method is described in more details in [8]. First, the system has to be written in a linear form in order to express the parameters. The main difference with [8] is the decomposition of the inertia between a constant term $\boldsymbol{I_{CB}}$ that needs to be estimated and $\boldsymbol{I_{SP}}$ being assumed known. Indeed, the solar panel inertias are often well characterized on ground. From the equation in the previous section, we obtain:

DOI: 10.13009/EUCASS2022-6092

$$-\dot{H}_{RW} - \Omega(t) \wedge H_{RW} = \left(\dot{\Omega}(t) + \Omega(t) \wedge \Omega(t)\right) \boldsymbol{I_{TOT}} - T_{ext} \quad (3)$$

$$g(t_k) = f(t_k) \boldsymbol{I_{TOT}} \quad (4)$$

At each time step t_k. Using eq. (2), the following expression is deduced :

$$g(t_k) - f(t_k) \boldsymbol{I_{SP}}(t_k) = f(t_k) \boldsymbol{I_{CB}} - T_{ext} \Rightarrow g'(t_k) = f(t_k) \boldsymbol{I_{CB}} - T_{ext} \quad (5)$$

In the basic instrumental variable method, the analytical solution is given by [14]:

$$I_{CB}^{IV} = [\sum_{k=1}^{N} \boldsymbol{Z^T}(t_k) f(t_k)]^{-1} [\sum_{k=1}^{N} \boldsymbol{Z^T}(t_k) g'(t_k)] \quad (6)$$

Where $\boldsymbol{Z}$ is the instrument that needs to respect properties given in [15].

Then, in order to be applicable to a gyroless satellite, and with the aim of reducing the variance, the following algorithm is applied [8]:

- Estimation of the derivative of the satellite attitude for a gyroless satellite
- Prefiltering of the functions g' and the regressor f for optimality of the IV method
- Constructions of augmented regressor and instrument (delayed regressor chosen) including the initial conditions and filter parameters
- Estimation of the parameters
- If needed, iterations until the algorithm has converged.

2.2 Unscented Kalman filter

The alternative method that has been implemented is based on a Kalman Filter. Since the dynamics equations of motion are nonlinear in state and parameter representation, special realizations of Kalman filters are required. The one chosen here is the Unscented Kalman Filter described below.

The estimated states are : $X = \begin{bmatrix} \Omega \\ I_{CB} \end{bmatrix}$ with I_{CB} the vector containing the six independent parameters of the matrix. Since the state Ω and the parameters I_{CB} are both estimated in the same algorithm, the method is called Joint Unscented Kalman Filter. The unscented transformation our work relies on is a method for calculating the statistics of a random variable through a nonlinear transformation. The different steps of this unscented transformation are explained in [13] and applied in our algorithm. Various parameters have to be tuned, which was done using trial and error. The initial state and the initial process covariance matrix have to be tuned, then the sigma points are calculated thanks to the process described in [13]. The propagation and measurement equations used for our application are described below.

The propagation model states:

$$X_{k+1/k} = \begin{bmatrix} \Omega_{k+1} \\ I_{CB_{k+1}} \end{bmatrix} = \begin{bmatrix} \Omega_k + \Delta t \left(\boldsymbol{I_{TOT_k}}^{-1}\right)\left(-\dot{H}_{RW_{k+1}} - \Omega_k \wedge (\boldsymbol{I_{TOT_k}} \Omega_k + H_{RW_{k+1}})\right) + \chi^{Q,x} \\ I_{CB_k} + \chi^{Q,w} \end{bmatrix} \quad (7)$$

With :

- $\boldsymbol{I_{TOT_k}} = \boldsymbol{I_{CB_k}} + \boldsymbol{I_{SP_k}}$
- $\chi^{Q,x}$ the noise on the state propagation model and $\chi^{Q,w}$ the noise on the parameter estimation model, sized by the covariance matrix $\boldsymbol{Q}$ constant.
- $\dot{H}_{RW_{k+1}}$ and $H_{RW_{k+1}}$ are the torque and angular momentum of the reaction wheels, input of the UKF
- Δt is the discretization time step

The advantage of the UKF is that there is no need to linearize this equation.

The measurement equation is :

$$M = \Omega_{k+1} + \chi^R \quad (8)$$

DOI: 10.13009/EUCASS2022-6092

With :

- M the measurement vector
- χ^R the noise associated with this equation, sized by the covariance matrix $\boldsymbol{R}$ chosen fixed.

The sigma point propagation can then take place using the method proposed in [6].

3. Choice of the observability methods

The observability of a system is defined as a measure of how well its internal states can be inferred from knowledge of its external outputs. In this specific case, the goal is to measure how well the inertia parameters can be estimated knowing the angular rate of the satellite.

Four metrics are considered to study the manoeuvres observability: the A-optimality, the D-optimality, the E-optimality and the Condition Number minimization [10], [11]. In [12], Nainer made use of them to design the best manoeuvre as input for the estimation. Differently, the focus is here on understanding what data are the most interesting to use as input for the inertia estimator. In this section, the four methods are briefly recalled.

Understanding how valuable a set of data is represents a common problem in the domain of parameter estimation. A typical approach is to use the Fisher Information Matrix [16], which is a measure of the amount of information that a variable x provides on the unknown parameter θ. From eq. (4), it can be demonstrated that the Fisher Information Matrix is given by:

$$\boldsymbol{I}(\theta) = \frac{f^T f}{\sigma^2} \tag{9}$$

With σ the variance of the noise vector (assumed random with zero mean) applying on eq. (4). Maximizing the Fisher Information Matrix eigenvalues corresponds to minimizing the lower bound of the variance estimates.
The four proposed methods aim at optimizing these variance estimates [10], [11]:

- D-optimality : this method computes the determinant of $f^T f$. The higher the better.
- E-optimality : it computes the minimum eigenvalue of $f^T f$. The higher the better.
- A-optimality : this criterion computes the trace of $(f^T f)^{-1}$. The lower the better.
- Condition Number: It corresponds to the ratio between the highest and the lowest singular value of the regressor matrix $\boldsymbol{f}$. It measures how much the output value of the function can change for a small change in the input argument. The lower the better.

These functionals are closely related to the Singular Value Decomposition (SVD) concept, and in particular, the E-optimality computes the minimal singular value. If a singular value is 0, then it means that there is one term (or combination of terms) on the inertia matrix that is not observable. By calculating the SVD, it is then possible to relate a low singular value to a combination of terms that are not observable. Often, the singular values are not exactly zero, thresholds have to be defined in order to consider a "sufficient" observability.

It is also possible to check only the observability on the diagonal terms if the non-diagonal terms are not that important.

From eq. (3) and (4), it can be noticed that f depends on the angular rate and its derivative. So the more the satellite is moving in the three directions during the analysed lapse of time, the more that interval is interesting for the estimation. To put it in another way, the four methods measure the amount of dynamics of the considered interval.

It has to be remarked that some maneuvers might exhibit an accentuate dynamic in a certain direction but none in the others. In this case, the methods will not point those particular maneuvers as interesting because some singular values will remain low. This of course reflects the intent of estimating all the parameters of the inertia matrix and shows the difficulty of finding the right span of data for the estimation. Various strategies can be applied: finding a maneuver

DOI: 10.13009/EUCASS2022-6092

with a sufficient observability, concatenating maneuvers with high observability along various axes, performing the estimation of only the observable inertia parameters for a given maneuver etc.

4. Application: Microcarb AOCS description

3.1 Microcarb mission

Foreseen to be launched in 2024, Microcarb will offer a global monitoring of the CO_2 surface fluxes, which will provide an insight onto the mechanisms governing exchanges between CO_2 sources and sinks, their seasonal variability, and their evolution in response to climate change.

In addition, Microcarb intends to lead the way towards the development of a future operational system able to accurately monitor global CO_2 emissions [17].

The concentration measurements will be performed by a passive Short Wave Infrared spectrometer. It will measure the solar light reflected by the Earth surface in the near infrared. In these wavelengths, the solar spectrum is modified by the CO_2 molecules in the atmosphere. The concentration is then deduced from the depth of the absorption lines in the measured spectra. The instrument also includes an imager designed to detect clouds which would corrupt the spectrometer measurements.

4.2 Pointing modes

To fulfill its mission of measuring the global CO_2 surface fluxes, four main mission acquisition modes have been developed. Thus, Microcarb is designed to measure the spectral radiance of the solar radiation reflected by Earth:

- At Nadir on land surfaces (Nadir Mode),
- At Glint point, where the sun light reflection is specular, on the oceans (Glint Mode),
- On calibration TCCON (Total Carbon Column Observing Network) stations (Fixed Target Mode). This mode requires a velocity ten times higher than orbital angular frequency, and an Absolute Pointing Error (APE) better than 1000 µrad.
- In order to improve spatial coverage and to get uncorrelated measurements, an across-track sight-changing mechanism is implemented in the instrument. This is used for the Scan mode which consists in gradually off pointing the line of sight from the Nadir.

In addition to this, probationary modes have been developed. Microcarb is not specifically designed to achieve these modes, but its capability to do so is evaluated. Two of these probationary pointing modes consists in demonstrating the ability to map CO_2 emissions at local scales, covering area from 40km x 40km (City mode) to 400km x 400km (Region mode). The City Mode consists in a pitch slew in order to pass 2 or 3 times on the city zone. This mode requires a velocity ten times higher than orbital angular frequency.

These innovative pointing modes require a challenging agility, and thus AOCS architecture evolutions, as described in [18].

4.3 AOCS normal mode

Microcarb AOCS inherits from the generic MYRIADE AOCS composed on the four following modes presented in [19].

DOI: 10.13009/EUCASS2022-6092

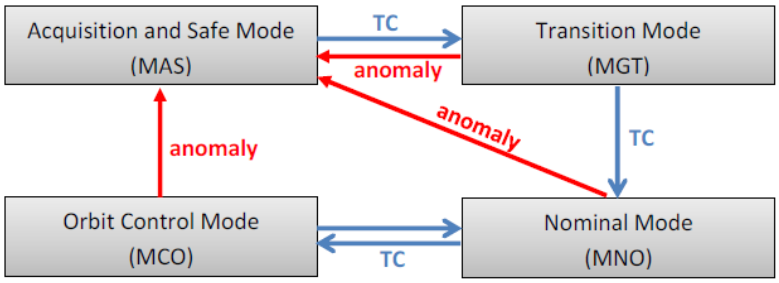

Figure 1: MYRIADE AOCS modes

To meet the performance requirements in normal mode, the generic Myriade control algorithms needed to be upgraded. The controller structure is an inheritance from Myriade. On Microcarb, the structured H-infinity method has been used to synthesize the controller, presented in [1]. This up-to-date method allows finding the optimum controller for given frequency constraints, while keeping the same controller structure.

As the controller bandwidth is limited by the wheels dynamics, in order to reduce the pointing error induced by the controller response time, a feed-forward command has been implemented. It consists in controlling the wheels in open-loop. The command is the angular momentum needed to follow the guidance profile. Thus the closed-loop controller only has to compensate for the errors around the target value and for the delays due to the wheels response time. The feed-forward control law is given by eq. (10) [18].

$$K_{ff} = G_{ff} \boldsymbol{I_{tot}} \dot{\Omega}(t + \Delta T) \tag{10}$$

Where :

- $\boldsymbol{I_{tot}}$ is the satellite inertia tensor,
- $\dot{\Omega}$ is the target acceleration,
- G_{ff} and ΔT are two tuning parameters to be optimized.

The dependence on $\boldsymbol{I_{tot}}$ is clearly visible in this control law.

4.4 AOCS Simulator

A highly representative simulation system is essential to develop and validate the AOCS architecture of a spatial system. MICROCARB simulator was developed in the CNES AOCS work environment called OCEANS using MATLAB© and SIMULINK©. OCEANS role is multiple:

- Technical legacy management
- Easier development of models
- Development and modification of simulators
- Scenarios generation and test launches
- Results exploitation

Microcarb simulator proposes different architectures, depending on the use:

- mono-mode structure: for development and validation of each mode;
- multi-modes structure: to test all the modes' transitions and failure detections and recovery action using the same principles.

The datasets for this study were generated with the MNO mono-mode simulator, using typical mission profiles.

5. Results on optimal guidance profiles

For the comparison of the identification methods, a total of 100 datasets were generated with dispersion of simulation parameters such as the orbital initial position, and the noise seeds in the sensors, but with a constant inertia matrix. The

DOI: 10.13009/EUCASS2022-6092

guidance profile is composed of manoeuvres along X, Y and then Z axes enabling a good observability on all axes. This guidance profile is however not realistic and is just studied to compare the identification methods.
Below are the results obtained with the two methods on average on the dataset.

Table 1: Estimation results on an optimal guidance profile

I_tot (kg.m²)	True value	IV estimation	IV relative error (%)	UKF estimate	UKF relative error (%)
I_xx	20.26	20.25	0.03	20.34	0.41
I_yy	23.25	23.25	0.00	23.46	0.91
I_zz	27.83	27.79	0.15	27.84	0.04
I_xy	-1.37	-1.36	1.03	-1.37	0.47
I_xz	-2.17	-2.17	0.01	-2.15	0.50
I_yz	-0.37	-0.38	3.31	-0.37	1.02

The performance of the estimation is very good, especially for the IV method and the diagonal terms. Since the non-diagonal terms have small absolute values, relative errors can be rapidly important while the results are still very good in absolute. The estimation of the IV method has been done using the velocity estimation of the on-board filter and not filtered from the quaternions data as proposed by [8] which slightly improved the results.
From this result, it can be concluded that the methods proposed can give very accurate estimations, if the input data is observable.

6. Observability analyses

6.1 Choice of the datasets

The baseline datasets used for this study consists in a typical mission day of Microcarb mission. This mission plan provides a chaining sequence of pointing modes (as described in section 3.2) and slew maneuvers. Figure 2 shows the guidance modes (top figure) and the angular rates (bottom figure) as a function of time. On the top figure, the y-label corresponds to the pointing modes identifiers: low numbers (i.e. < 10) are associated to the mission modes of the satellite (NADIR, GLINT, FIXED TARGET and so on) and high numbers (>30) correspond to slew maneuvers.

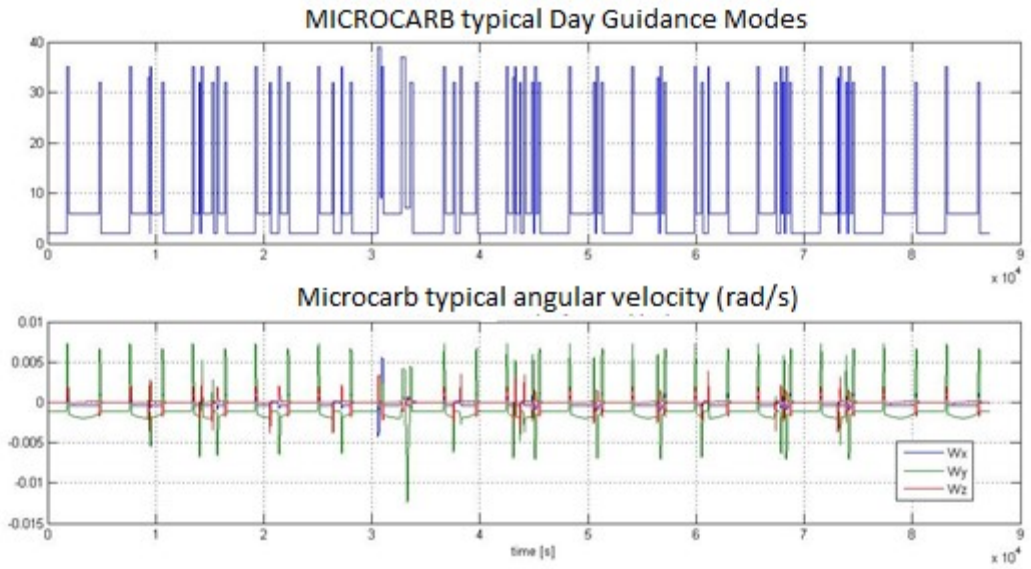

Figure 2 : Guidance Modes and Angular Rate Typical Day MICROCARB

A first high-level analysis of this dataset gives some preliminary information useful for the observability analysis:

- the excitation is preponderant on the Y-axis (mainly during the slew maneuver). Consequently, the estimation might be more precise for the parameters linked to Y.

DOI: 10.13009/EUCASS2022-6092

- It seems that a significant manoeuvre on X only happens at a precise moment of the day ($t \sim 3.1 \times 10^4\ s$). That might result in a good estimation of the related inertia parameters for that particular lapse of time.
- Finally, there are quite a few intervals when the angular rate is constant. These periods do not give useful information and can even decrease the performances of the estimation.

Separating the day in intervals on which to study the observability is necessary since considering the whole day for the estimation would lead to imprecise and slow convergence of the UKF method or inaccuracy and pointless slowness for the IV method. Indeed, when the observability is low, the estimation result is less accurate because the noise become more important than physical movement and can be even wrong if there is no observability on one or more axes. In addition, all the data have the same weight in the algorithms, and so a minimization of the errors is done in the IV, and if many data carry low observability, the final performance will be decreased. The impact can be even more harmful for the UKF if the estimation finishes on a low-observability profile, the final estimation can be wrong. Thus it is important to select only the periods when useful information can be deduced. This preliminary analysis is essential to decide how to divide the data before launching the observability algorithms.

The goal is thus to find the best intervals in both quality and fastness on which to run the estimation. In the following chapter, different approaches to cut the day are suggested. In all cases, the observability is studied and the estimation is launched.

6.2 Data combination methods

Three different scenarios have been considered using the data previously presented:

- Scenario #1: the typical day has been cut in smaller portions and the observability has been studied on each of these groups.
  The initial objective of this scenario was to analyze the whole sequence. However cutting periods of low dynamic (such as long NADIR periods) proved to be necessary because it can lead to divergence or wrong estimation as well as making the estimation longer without adding extra information.
  Short periods of flat dynamics however are kept, because they will not disturb the algorithm convergence process.
  This division led to the definition of 15 groups.

- Scenario #2: each mode observability is studied individually.
  The purpose of this scenario is to identify the most interesting modes in terms of observability.

- Scenario #3: a fictitious sequence of guidance modes is created by pasting together the most interesting guidance modes.
  The best 10 guidance modes identified in the previous scenario are pasted together to observe if a very precise estimation can be ensured.

6.3 Results and comparisons

Scenario #1 results

The four methods presented in section 1.3 are applied to the 15 groups. Clearly, the 6^{th} group appears to be the densest of information by far according to all the four methods: As an example, Figure 3 shows the results for the A-optimality method.
This result is partly confirmed by comparing the observability results with the estimation errors in Figure 4 and Figure 5. For both IV and UKF methods, it can be observed that the $\boldsymbol{I_{yy}}$ parameter is always well estimated compared to the others. As previously stated, the satellite dynamics are preponderant on the Y axis and such a result was expected. Concerning the results for $\boldsymbol{I_{xx}}$ and $\boldsymbol{I_{zz}}$, the UKF results appear to be in line with what the observability study is showing and the 6th group presents the overall best estimation. In particular, it can be said that the 6th group ensured the most accurate estimation of the three parameters at the same time. However, with the IV method, whereas the 6th group appears to have a good accuracy in the estimation, the 3rd, 4th and 5th groups also present very little errors, in some cases even smaller than the 6th group.

DOI: 10.13009/EUCASS2022-6092

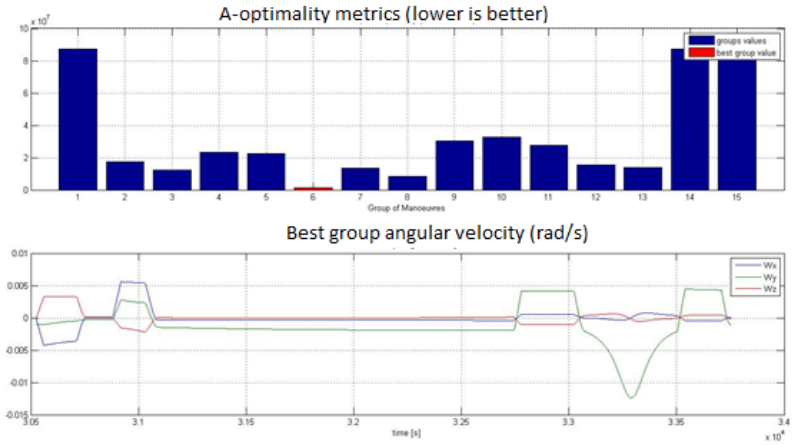

Figure 3 : A-Optimality Method vs Groups of Manoeuvers

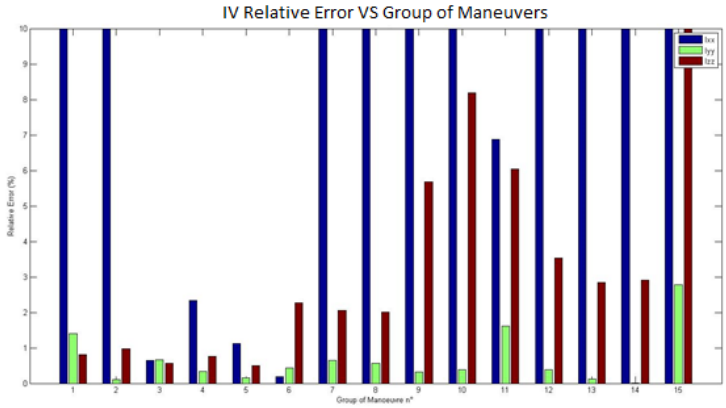

Figure 4 : IV Relative Error vs Group of Manoeuvres

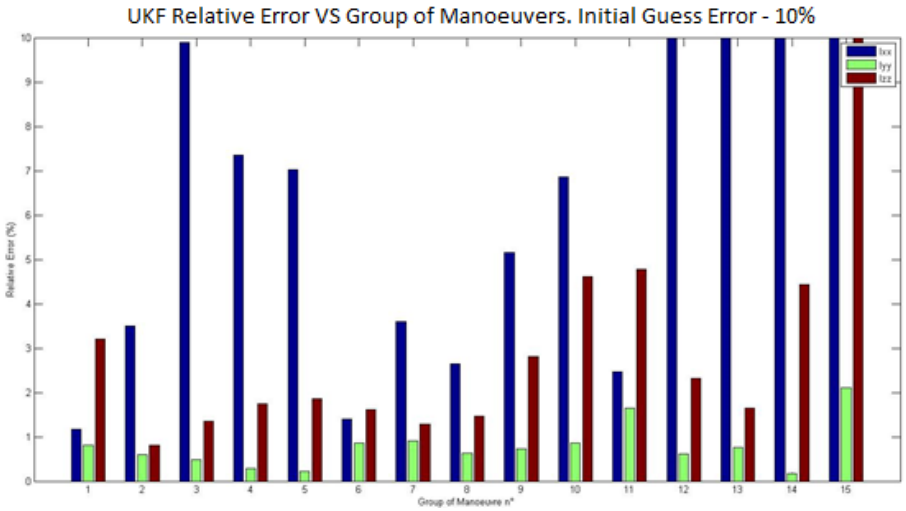

Figure 5 : UKF Relative Error vs Group of Manoeuvres

These first results lead to a first set of analyses:

- Why do all the observability methods point to the 6th group as the best by far?

As previously explained, the four methods make use of the Regressor matrix f as input. Thus, the more the excitation is in all the three directions, the more the observability methods will consider a certain guidance mode as interesting. It can be observed that the 6^{th} is the one that presents the most relevant change of velocities on X and Z. Among the

DOI: 10.13009/EUCASS2022-6092

manoeuvres of this interval, one can find the FIXED TARGET (guidance mode n°7) mode, which is possibly the manoeuvre with the greatest amount of dynamics. All the 15 groups present a good amount of information on the Y-axis and this is coherent with the accuracy of the I_{yy} estimation for all of them. However, in most of the cases there is no relevant change of velocity on X and Z. This explains why the 6th group appears to be the densest of information.
In a way, the four observability methods measure how the excitation is spread on the three axis. To rephrase it, even if on a certain interval of the day there is a great excitation on one axis, if there is no much dynamic on the others, then the observability methods will not point it out as a good one.

- Why does the IV method present very good estimation results also for other groups of manoeuvres?

In particular, the focus is on the third, fourth and fifth group, which lead to a precise estimation but are not interesting according to the observability methods. If compared to the other groups they do not present greater excitations. Exactly as the others, they do have an interesting dynamic on the Y-axis but no more than the others on Z and X. The third one has a slightly more aggressive dynamic on the Z-axis but nothing more than the 12th or 13th group, which do not lead to a good estimation and do not result to be interesting according to the observability methods. It should be noted that the IV method is the most robust among the two identification methods.

As the core of the study is understanding if the observability methods outputs ensure good estimations, the primary objective remains studying the performances of the IV and the UKF on the 6th group and it has been shown that the observability methods pointed an interval that guaranteed a precise estimation.

The UKF seems more in-line with the observability study, however it should be noted that it is not expected that the observability results give a measure of the performance of the estimation. Indeed, if the whole day is taken in input of the estimation algorithm, then the observability result will show a high observability while the performance will be bad because there will be a lot of points that are unobservable for some inertia parameters, thus creating an inaccuracy in the results. The information is present but the methods are not able to exploit it optimally.
The observability is a necessity for estimation, but as seen with the IV, lower criteria values can be enough for the IV. These criteria are statistical because linked to the variance, even if the result is good here it does not mean it will always be the case, since the uncertainty on this estimation is higher than with a group of manoeuvres with a lower variance/higher observability.

Scenario #2 results

After these analyses, the observability methods were applied to each individual pointing mode, in order to understand why the 6th group gave better results.

The best modes are the slew manoeuvres and the FIXED TARGET. The result is consistent with what we could expect from observing the velocity profiles for these guidance modes. Also, it can be observed that the 6th group previously analysed is the only one with the fixed target, in addition to some slew manoeuvres. This explains its higher observability.

It is interesting to underline that the same transition modes are not always equally observable. This remarks the fact that even if the scope of each guidance mode is the same (for example to make the satellite ready for NADIR), the execution is not always exactly equal, thus the amount of information varies even between two same guidance modes. Hence, it cannot be stated which guidance mode is the best overall but it is necessary to apply the observability methods on each Microcarb day.
In any case, NADIR and GLINT guidance modes never appear among the best ones. This is consistent with their flat velocity profiles.

Scenario #3 results

Finally, the best 10 guidance modes are pasted together to observe if a very precise estimation can be ensured.

The type of profile that is expected is shown in Figure 6. As it can be observed, the modes present considerable excitations especially on Y and Z, whereas on the X-axis the dynamics are less pronounced in most of the cases. The Figure shows the sequence resulting from the E-Optimality observability method this time.

DOI: 10.13009/EUCASS2022-6092

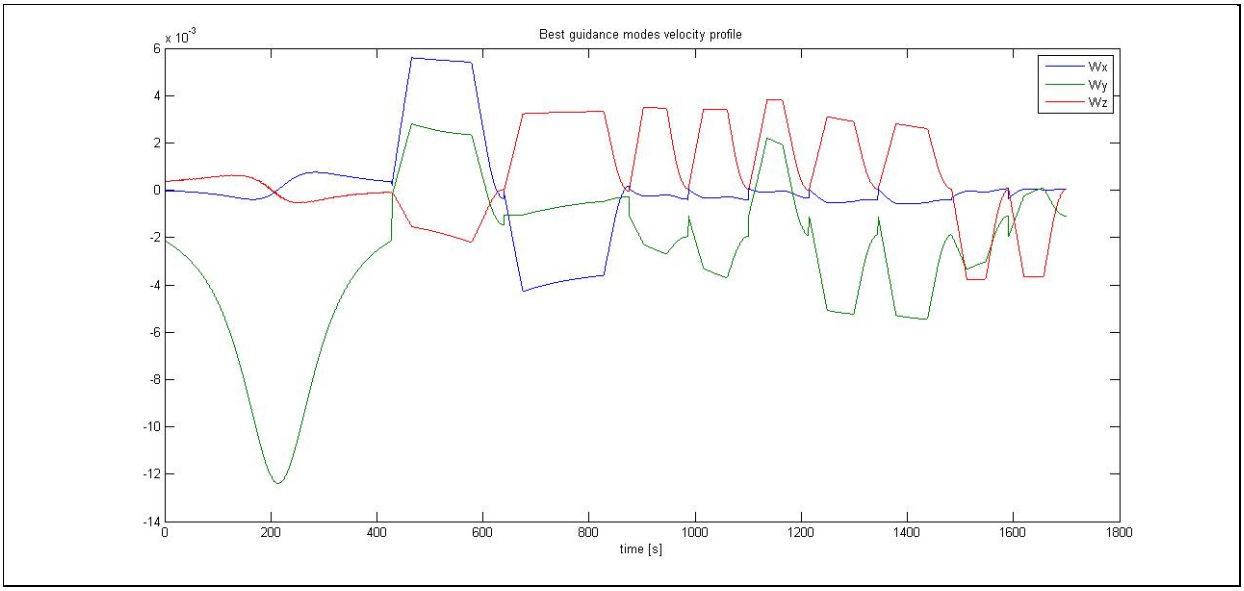

Figure 6 : E-Optimality sequence (velocity profile in rad/s)

First of all, each observability method has been tried on the sequences resulting from pasting the best manoeuvres according to each of the four methods. Results are shown in Table 2. As previously underlined, each observability method proposes a slightly different optimal of best guidance modes, thus results consider the four methods. For each method the best sequence is in bold. The ideal manoeuvre is the one considered in section 5.

Table 2 : Observability results on the best sequences created according to each observability method

	A-Optimality (↓) $\times 10^{5}$	**D-Optimality (↑)** $\times 10^{-26}$	**E-Optimality (↑)** $\times 10^{-5}$	**Condition Number (↓)**
A best GMs	**1.67**	**1.98**	1.31	3.23
D best GMs	1.77	1.23	1.25	3.09
E best GMs	1.71	1.35	**1.36**	**3.07**
CN best GMs	1.75	1.18	1.33	3.16
Ideal maneuver	2.22	2.47×10^{11}	1.35	1.44

It can be observed that the most interesting sequences appear to be the one proposed by the E-Optimality and the A-Optimality methods. The values obtained by the D-optimality are very small because they are the multiplication of the singular values, themselves depending on the velocity of the satellite. To compare groups of manoeuvres that can have various durations, one idea was to normalize these criteria for instance with the duration of the manoeuvres or with respect to an ideal manoeuvre. This axis of thinking can still be researched.

Table 3 shows the observability results of the 6th group compared to those of the fictitious sequence created according to the E-Optimality method, all normalized by the results of the reference manoeuvre used in section 5. As a result, the more the ratio is close to 1, the more the sequence of modes is expected to be interesting. Since the A-Optimality and the Condition Number are better if small, the ratio is expected to be above one if the reference manoeuvre is better. The opposite will happen for the D and the E Optimality methods.

Table 3 : 6th group VS E-Optimality best sequence

	Ratio A-Optimality	**Ratio D-Optimality**	**Ratio E-Optimality**	**Ratio Condition Number**
6th group	4.54	0.070	0.06	5
Sequence	0.5182	250	1.0462	2.0467

The 6th group gives better results on the observability metrics. However, the duration of the sequences is not the same and the 6th group is longer than the others.

DOI: 10.13009/EUCASS2022-6092

Finally, the estimation results are shown in the following table for the IV and the UKF methods by using as input the four sequences generated by the observability criteria.

Table 4 : 6th group VS E-Optimality best sequence

Relative Error (%)	I_{xx}		I_{yy}		I_{zz}	
	IV	***UKF***	***IV***	***UKF***	***IV***	***UKF***
A-Optimality	2.10	2.10	1.21	5.48	1.41	2.01
D-Optimality	1.96	1.79	0.85	3.28	0.49	1.97
E-Optimality	**1.34**	**0.62**	**1.16**	**1.70**	**0.66**	**2.76**
Condition Number	0.35	12.89	1.17	3.39	1.46	4.17

As it can be observed, the IV ensures a very low error (the highest is 2.1%). On the contrary, the UKF did not always work at its best and the error is above 5% in two cases. The overall best sequence has been highlighted and is the one created by the E-Optimality method. The fact that the UKF is not always precise can be explained considering that the UKF filter is an iterative method that improves its estimation at each time step. For this reason, it cannot be the optimal method when dealing with discontinuity. Because of the guidance modes copy-paste process adopted to create the sequence, the resulting sequence presents many discontinuities that degrade the estimation by such a method. Also, only the final value is considered and can be subject to less observable final periods or perturbations, contrary to the IV which has an averaging process decreasing the impact of noisy estimates.
Figure 7 shows that in correspondence of these gaps, the estimation is badly affected for the UKF. This is evident for instance between the first and the second guidance mode for the I_{yy} estimation. In addition, as explained before, only one manoeuvre is well observable in X and enables a convergence towards the true value, but after it, there is a drift of the estimation.

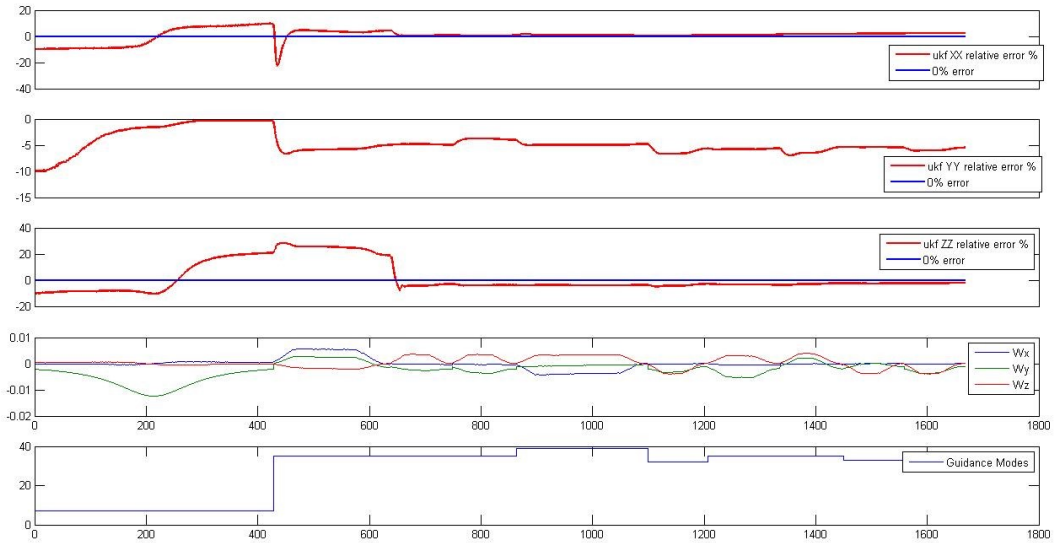

Figure 7 : UKF Relative Error (%) Convergence on the A-Optimality Sequence

The most important consideration is anyway the comparison with the estimation results of the 6th group. As it can be deduced, despite the remarkable better results in terms of observability, the estimation precision is not significantly improved, Indeed, the 6th group was way longer than the fictitious sequence. The best is to find a compromise in length of the group and density of dynamics, or add more guidance modes to the sequence or even improve the algorithms so that they become less sensitive to data with small observability.

The fact that the E-optimality criteria gives the best results is not surprising because it maximizes the observability on the less-observable parameter to be identified. If the criteria value is acceptable, then all the information is available

DOI: 10.13009/EUCASS2022-6092

for estimation. The A-optimality and D-optimality, using the trace and the determinant of matrices derived from the regressor, give rather a mean value of observability where disparities between the minimal and maximal singular values can be hard to check. On the other side, the condition number gives this information, but it is not known if the minimal value has a sufficient value to be considered "observable". It is then possible to refine the analysis, depending on the need for instance to a certain value for the observability of the minimal singular value while ensuring a good condition number.

7. Conclusion

This paper presented the study on the observability of the input data for the inertia satellite estimation with a particular focus on the MICROCARB mission. The need for such a tool has proven crucial especially when no specific guidance mode for inertia estimation is planned. Results have shown that the observability outputs used as input on the programme can ensure to reach the sub 5% relative error goal required for the MICROCARB mission and that in this case it has been easily possible to keep it below 2%.

The various criteria for observability gave different results, however their consistency is an important feature when selecting the best manoeuvres for the estimation. The two identification methods gave a priori good results when a specific manoeuvre is considered, nevertheless the difficulty of finding "good" data among a set of manoeuvres is not easy. The IV method has proven more robust than the UKF in the study presented, taking advantage of the fact that it uses all the data at once to find the parameter values.

Validation has been performed on different days of simulated data, not presented here, but increasing the confidence in the analysis.

Some perspectives stand out of this paper:

- During the study, the possibility to add weights on the guidance modes of the sequences has been considered. While the IV method lends itself well to this kind of analysis, the implementation on the UKF is not that trivial since it required changing the covariance values in a way that did not compromise the stability of the UKF.
- Normalisation of the observability metrics should be researched.
- In addition, since the actuator alignments directly affect the generated control torque, it could be of great interest to ensure a precise estimation of these parameters as already proposed by Nainer in [8].

To conclude, this study enabled us to have a process for inertia estimation based on observability analyses and then identification algorithms that can be of great help to calibrate the inertias during the first weeks of life of a satellite.

References

[1] Genin, F. and F. Viaud. 2018. An innovative control law for MICROCARB microsatellite. In : *AAS GNC 2018*, Breckenridge.

[2] Lee, A. Y. and J.A. Wertz. 2002. In-flight estimation of the Cassini spacecraft's inertia tensor. *Journal of spacecraft and rockets*. 39(1): 153–155.

[3] Manchester, Z. R. and M. A. Peck. 2017. Recursive inertia estimation with semidefinite programming. In : *AIAA Guidance, Navigation, and Control Conference*. 1902.

[4] Wilson, E., C. Lages, and R. Mah. 2002. On-line gyro-based, mass-property identification for thruster-controlled spacecraft using recursive least squares. In : *The 2002 45th Midwest Symposium on Circuits and Systems*. 2 : II–II.

[5] Yoon, H., K.M. Riesing and K. Cahoy. 2017. Kalman Filtering for Attitude and Parameter Estimation of Nanosatellites Without Gyroscopes. *Journal of Guidance, Control and Dynamics*. 40(9): 2272-2288.

[6] Sekhavat, P., M. Karpenko and I. Ross. 2009. UKF-based spacecraft parameter estimation using optimal excitation. In : *AIAA Guidance, Navigation, and Control Conference*. 5786.

[7] Kornienko, A., P. Dhole, R. Geshnizjani, P. Jamparueang and W. Fichter, W. 2017. Determining Spacecraft Moment Of Inertia Using In-Orbit Data. In : *GNC 2017: 10th international ESA conference on Guidance, Navigation and Control Systems*, Salzburg, Austria.

DOI: 10.13009/EUCASS2022-6092

[8] Nainer, C. 2020. In-Orbit Data-Driven Parameter Estimation for Attitude Control of Satellites. PhD Thesis. Université de Lorraine.
[9] Chaturvedi, N. A., D.S. Bernstein, J. Ahmed, F. Bacconi and N.H. McClamroch. 2006. Globally Convergent Adaptive Tracking of Angular Velocity and Inertia Identification for a 3-DOF Rigid Body. *IEEE Transactions on Control Systems Technology*. 14(5): 841–853.
[10] Franceschini, G. and S. Macchietto. 2008. Model-based design of experiments for parameter precision: State of the art. *Chemical Engineering Science*. 63(19): 4846–4872.
[11] Walter, É. and L. Pronzato. 1990. Qualitative and quantitative experiment design for phenomenological models - a survey. *Automatica*. 26(2): 195–213.
[12] Nainer, C., M. Gilson, H. Garnier, C. Pittet and H. Evain. 2020. Design of satellite maneuvers for inertia parameter estimation. *21st IFAC World Congress*. *IFAC-PapersOnLine*. 53(2):14894-14899.
[13] Wan, E. and R. Van Der Merwe. 2000. The Unscented Kalman Filter for Nonlinear Estimation. *IEEE Transactions*.
[14] Söderström, T and P. Stoica. 1983. *Instrumental variable methods for system identification, Lectures Notes in Control and Information Sciences*. Springer-Verlag, Berlin.
[15] Young, P. C. 2011. *Recursive estimation and time-series analysis: An introduction for the student and practitioner. 2nd*. Springer.
[16] Goodwin, G. C and R. L. Payne. 1977. Dynamic system identification: experiment design and data analysis. *Academic press*.
[17] P. Veronique and al. 2012. A new space instrumental concept based on dispersive components for the measurement of CO2 concentration in the atmosphere. *ICSO.*
[18] Rineau, G., F. Genin and S. Delavault. 2020. Microsatellite Aocs Design For The Agile Mission Microcarb. *GNC 2021: 11th international ESA conference on Guidance, Navigation and Control System.*
[19] Le Du M., J. Maureau and P. Prieur. 2002. Myriade: an adaptative AOCS concept. *GNC 2002: 5th international ESA conference on Guidance, Navigation and Control System*.